Contents lists available at ScienceDirect

Current Research in Microbial Sciences

Alpaca-derived nanobody targeting the hydrophobic pocket of the HIV-1 gp41 NHR broadly neutralizes HIV-1 by blocking six-helix bundle formation

Lujia Sun [a,1], Bo Chen [b,1], Xianbo Liu [b], Yun Zhu [c], Guangxu Zhang [a], Xiaoxing Liang [a], Lixiao Xing [a], Wei Xu [a], Shibo Jiang [a,*], Xinling Wang [a,*]

[a] *Shanghai Institute of Infectious Disease and Biosecurity, Key Laboratory of Medical Molecular Virology (MOE/NHC/CAMS), School of Basic Medical Sciences, Shanghai Frontiers Science Center of Pathogenic Microbes and Infection, Fudan University, Shanghai, China*
[b] *Chengdu NBbiolab. CO., LTD, SME Incubation Park, 319 Qingpi Avenue, Chengdu, China*
[c] *National Key Laboratory of Biomacromolecules, CAS Center for Excellence in Biomacromolecules, Institute of Biophysics, Chinese Academy of Sciences, Beijing, China*

A R T I C L E   I N F O

A B S T R A C T

The highly conserved hydrophobic pocket region of HIV-1 gp41 NHR triple-stranded coiled coil is crucial for the binding of CHR to NHR to form a six-helix bundle (6-HB). This pocket is only exposed instantaneously during fusion, making it an ideal target for antibody drug design. However, IgG molecule is too big to enter the pocket during the fusion process. Therefore, to overcome the steric hindrance and kinetic obstacles caused by the formation of gp41 pre-hairpin fusion intermediate, we obtained nanobodies (Nbs) targeting NHR by immunizing alpaca with an NHR-trimer mimic. Specifically, we identified a Nb, Nb-172, that exhibited potent and broadly neutralizing activity against HIV-1 pseudoviruses, HIV-1 primary isolates, and T20-resistant HIV-1 strains. In addition, the combinatorial use of mD1.22 and Nb-172 exhibited synergism in inhibiting HIV-1 infection inactivating cell-free virions. Nb-172 can competitively bind to the hydrophobic pocket of gp41 NHR to inhibit 6-HB formation. These findings suggest that Nb-172 merits further investigation as a potential therapeutic for HIV-1 infection.

1. Introduction

Acquired immunodeficiency syndrome (AIDS) caused by the human immunodeficiency virus-1 (HIV-1) has remained a significant public health challenge over the past 40 years. Even though antiretroviral therapy (ART) has brought a glimmer of hope to HIV-infected patients (Palella et al., 1998; Simon, et al., 2006), strict compliance is necessary since an interruption of ART will lead to a rapid rebound of HIV-1 and the continuous progression of disease owing to the phenomenon of persistent latent reservoir (Finzi, et al., 1999). Additionally, lifelong treatment usually leads to the accumulation of toxicity and drug resistance (Wittkop, et al., 2011). However, studies in humanized mice have shown that monoclonal antibody therapy can lead to prolonged inhibition of HIV-1 infection, even after the cessation of ART, suggesting that antibodies may play a role in treatment aimed at achieving HIV-1 remission (Halper-Stromberg, et al., 2014).

The development of potent, broadly neutralizing antibodies offers novel approaches for preventing, treating, and curing AIDS (Caskey, et al., 2019). To date, hundreds of HIV-1-specific monoclonal antibodies with broadly neutralizing ability have been reported, and some have been approved to enter the clinical stage, such as 3BNC117 (Scheid, et al., 2011) and 10–1074 (Mouquet, et al., 2012). However, most of these antibodies targeted mutation-prone antigenic sites exposed on the surface of gp120 and gp41, thus leading to the production of resistant strains (Zacharopoulou, et al., 2022).

During the process of infection, HIV-1 first binds to receptor CD4 and co-receptor CCR5 or CXCR4 through gp120, which induces a conformational change of gp41 that allows the fusion peptide (FP) of gp41 to be released and inserted into the target cell membrane. After this, the N-terminal heptad repeat (NHR) forms a trimeric coiled-coil structure, leading to the exposure of a conserved hydrophobic pocket on its surface, followed by reversal and tight binding of the extracellular C-

---

terminal heptad repeat (CHR) to the NHR trimer, or, more specifically, the hydrophobic pocket, to, in turn, form a stable 6-HB. This activity culminates in membrane fusion between target cell membrane and viral envelope (Chan, et al., 1997; Lu, et al., 1997; Weissenhorn, et al., 1997). Thus, it can be seen that the hydrophobic pocket of gp41, which corresponds to residues 568–579 of HIV-1 HXB2 (Bruun, et al., 2023), plays a key role in the fusion process. The characteristics of instantaneous appearance and exposure of the hydrophobic pocket during fusion make it difficult for pre-existing antibodies to induce its mutation (Lu, et al., 1997). As such, the hydrophobic pocket becomes an optimal target for antibody drug design. Ironically, however, exposure of the pocket region also makes it subject to such obstacles as steric hindrance and the kinetics of HIV Env-mediated fusion. Therefore, it is difficult for IgG (approximately 150 KD) to enter and play a neutralizing role (Eckert, et al., 2008; Sabin, et al., 2010). This dilemma is a key scientific issue in developing anti-HIV antibody drugs that can specifically target the hydrophobic pocket region of the NHR trimer and easily enter this region.

In fact, some antibody fragments have been designed to replace full-length monoclonal antibodies, including antigen-binding fragments (Fab) and single-chain variable fragments (scFv)(Caillat, et al., 2020). For example, D5 targeting the gp41 NHR is more potent as an scFv than as a full-length IgG in preventing the infection of different HIV isolates (Eckert, et al., 2008; Miller, et al., 2005). Furthermore, HK20-scFv showed the highest potency in complete HK20 IgG, HK20-based Fab, and scFv (Sabin, et al., 2010). Interestingly, apart from conventional antibodies, camels produce heavy-chain-only antibodies, which contain one single variable domain (VHH) rather than two variable domains (VH and VL), designated nanobody (Nb), that makes up the equivalent of Fab of traditional antibody IgG (Hamers-Casterman, et al., 1993; Wrapp, et al., 2020). Although they represent only about one-tenth of traditional antibodies, nanobodies still retain the specificity and affinity of traditional antibodies (Hanke, et al., 2020). Compared with human VH antibodies, nanobodies have a longer CDR3 able to form a disulfide bond with the adjacent CDR2 or CDR1 region to stabilize its structure. This elongated CDR3 loop exhibits greater structural flexibility, and can penetrate cavities on antigens, and may even have the capacity to specifically recognize hidden epitopes (De Genst, et al., 2006; Liu, et al., 2021). Their advantageous biophysical properties have led to the evaluation of several nanobodies as therapeutics against some pathogens (Cunningham, et al., 2021; Sarker, et al., 2013). However, no nanobodies are currently approved as HIV-1 therapeutics for clinical trials.

Here, we reported some anti-HIV-1 nanobodies isolated from an alpaca that was immunized with a gp41 NHR-trimer mimic. These nanobodies showed high binding affinity to the NHR-trimer protein and anti-HIV-1 activity. Among them, Nb-172 exhibited potent and broadly neutralizing activity against HIV-1 pseudoviruses, HIV-1 primary isolates, and T20-resistant HIV-1 strains. In addition, the combinatorial use of mD1.22 and Nb-172 exhibited synergism in inhibiting HIV-1 infection and inactivating cell-free HIV-1 virions. The anti-HIV-1 activity of Nb-172 is achieved by binding to the hydrophobic pocket of NHR to inhibit 6-HB formation, and it is the first reported nanobody targeting this region. The structural prediction shows that Nb-172 blocks the binding of CHR to NHR, mainly through the interaction between its CDR3 and residues 557–579 of NHR. These results suggest that Nb-172 merits further investigation as a potential therapeutic for HIV-1 infection.

2. Materials and methods

2.1. Cells and viruses

Expi293F, 293T, U87, MT-2, and CEMx174 5.25 M7 cells were all obtained from the American Type Culture Collection (ATCC). TZM-b1 cells were obtained from the NIH AIDS Reagent Program and stocked in our laboratory. Expi293F cells were cultured in SMM293-TII expression medium (Sino Biological, China), while MT-2 and CEMx174 5.25 M7 cells were cultured in RPMI-1640 medium containing 10 % fetal bovine serum (FBS). The 293T, U87 and TZM-b1 cells were cultured in DMEM with 10 % FBS. Viruses used in this study were obtained from the NIH AIDS Reagent Program.

2.2. Alpaca immunizations with covNHR-VQ

Alpaca immunizations were conducted by NBbiolab Co., Ltd. Immunogenic protein covNHR-VQ was overexpressed and purified, as described previously (Jurado, et al., 2019). Briefly, the sequence of covNHR-VQ was cloned into a pComb3x vector with a 6 × His-Tag in C-terminal and expressed in *E. coli* HB2151 cells. Bacterial transformation with expression plasmid was amplified at 30 °C for 12 h under the induction of IPTG at a final concentration of 0.1 mM. The supernatant of covNHR-VQ was purified by Ni-NTA (Smart-Lifesciences, China), and the protein was concentrated by ultrafiltration and redissolved in PBS. The purity of covNHR-VQ was detected by SDS-PAGE with a purity > 95 %. One alpaca was injected intramuscularly with a mixture of 0.5 mg covNHR-VQ and Freund's complete adjuvant. In the following 3rd, 6th, and 9th week, a mixture of 0.25 mg covNHR-VQ and Freund's incomplete adjuvant was injected into the alpaca, respectively, for booster immunizations. Alpaca serum was collected after every immunization for titer detection.

2.3. Enzyme-linked immunosorbent assay (ELISA)

ELISA was used to quantify antigen-specific immunoglobulin titer in alpaca serum. Briefly, 2 μg/mL covNHR-VQ were coated on wells of a 96-well polystyrene plate at 4 °C overnight. The plate was blocked with 5 % nonfat milk at 37 °C for 2 h before the inactivated alpaca serum was added. After incubation at 37 °C for 1 h, the plate was washed with PBST and then incubated with HRP-conjugated Anti-Alpaca IgG at 37 °C for 0.5 h. TMB (3,3′, 5,5′-tetramethylbenzidine) and H_2O_2 were used to visualize the enzyme-linked reaction.

To quantify the affinity of nanobodies to NHR trimeric protein or NHR-derived peptide, 2 μg/mL N63-trimer protein or 5 μg/mL IQN17 peptide were coated on wells of a 96-well polystyrene plate at 4 °C overnight. The plate was blocked with 5 % nonfat milk at 37 °C for 2 h before diluted nanobodies were added. After incubation at 37 °C for 1 h, the plate was washed with PBST and then incubated with HRP-conjugated 6*His Tag Monoclonal Antibody (Proteintech, China) at 37 °C for 0.5 h. TMB and H_2O_2 were used to visualize the enzyme-linked reaction.

We measured the competitive binding of CHR-derived peptides and Nb-172 to NHR trimer. Briefly, 2 μg/mL N63-trimer protein was coated on wells of a 96-well polystyrene plate and incubated at 4 °C overnight. The plate was blocked with 5 % nonfat milk at 37 °C for 2 h. Serially diluted C34 and T20 peptides were incubated with 1 μM Nb-172, and then the mixture was transferred to the ELISA plate (50 μL/well) and incubated at 37 °C for 1 h. After washing with PBST three times, HRP-conjugated 6*His Tag Monoclonal Antibody was added and incubated at 37 °C for 0.5 h. TMB and H_2O_2 were used to visualize the enzyme-linked reaction.

2.4. Phage library construction and clone selection

Phage library construction and nanobody expression were conducted by NBbiolab Co., Ltd. Briefly, peripheral blood of alpaca was collected after the 4th immunization, and peripheral blood mononuclear cells (PBMCs) were isolated using lymphocyte separating medium. Total RNA of PBMC was extracted by Trizol (Thermo Fisher, USA) and reverse transcribed by PrimeScript™ II 1st Strand cDNA Synthesis Kit (Takara, Japan) to synthesize cDNA. Then the nanobody gene fragment was amplified by nested PCR, and the products were cleaved with SfiI (NEB, USA) before insertion into the pComb3xss vector. The ligation product was transformed into *E. coli* TG1 cells to construct a nanobody phage

library against covNHR-VQ.

ELISA was used to screen positive phages. Briefly, 5 µg/mL covNHR-VQ were coated on wells of a 96-well polystyrene plate at 4 °C overnight. The plate was blocked with 3 % OVA-PBS at 37 °C for 2 h before adding the nanobody phage library. After incubation at 37 °C for 1 h, the plate was washed with PBST to wash away unbound phages, and 100 µL Gly-HCl were used for elution. Then the eluant was neutralized with Tris–HCl in the first and successive screening rounds. After three rounds of screening, 192 clones were randomly selected for monoclonal phage identification by ELISA. Briefly, 2 µg/mL covNHR-VQ were coated on wells of a 96-well polystyrene plate at 4 °C overnight. The plate was blocked with 5 % nonfat milk at 37 °C for 2 h before the addition of the phage culture supernatant. After incubation at 37 °C for 1 h, the plate was washed with PBST and then incubated with HRP-conjugated Anti-M13 Bacteriophage at 37 °C for 0.5 h. TMB and H_2O_2 were used to visualize the enzyme-linked reaction.

The nanobody gene fragment was cloned into an expression vector with a $6 \times$ His in the C-terminus. The recombinant plasmid was transformed into *Bacillus*, and the monoclonal colonies were activated in MT medium at 37 °C. After 4 h, the positive clones were identified by PCR, transferred to MTN medium at a ratio of 1:200, and cultured at 30 °C for 72 h. The supernatant was collected by centrifugation at 10,000 g for 10 min and was purified by Ni-NTA. The protein was concentrated by ultrafiltration, and the buffer was replaced with 0.1 M $NaHCO_3$ (pH 8.3). The purity of nanobodies was detected by SDS-PAGE with a purity > 90 %.

2.5. Inhibition of HIV-1 pseudovirus infection

Stocks of single-round-infection HIV-1 Env pseudovirus were produced by co-transfecting 293T cells with one volume of HIV-1 Env expression plasmid and two volumes of HIV-1 backbone plasmid (pNL4–3.Luc.R-E-) using VigoFect Transfection Reagent (Vigorous Biotechnology, China). After incubating at 37 °C for 8 h, the supernatant was replaced with fresh DMEM containing 10 % FBS. Culturing continued for another 48 h, and then the supernatants containing HIV-1 pseudoviruses were collected. To detect neutralizing activity, TZM-b1 cells were seeded into wells of a 96-well plate (10^4 cells per well) in advance. Nanobodies and D5 scFv were serially diluted in DMEM, followed by incubation with HIV-1 pseudoviruses at 37 °C for 0.5 h. Then the mixture was transferred into TZM-b1 cells. After 12 h, the mixture was replaced with fresh DMEM containing 10 % FBS. After culturing for another 48 h, the cells were lysed with cell lysis buffer (Promega, USA), and luciferase activity was detected with the Luciferase Assay System (Promega, USA).

2.6. Inhibition of HIV-1 infection

Inactivated alpaca sera, or nanobodies, were diluted in wells of a 96-well plate and incubated with 100TCID$_{50}$ HIV-1 at 31.5 °C (only for detection of alpaca serum neutralization) or 37 °C for 0.5 h before MT-2 cells or CEMx174 5.25 M7 cells were added to the mixture. MT-2 cells and CEMx174 5.25 M7 cells were used as target cells for the X4 and R5 virus, respectively. To test the mD1.22/Nb combination, the ratio of mD1.22 and VHH in the combination was calculated based on their own IC50, as previously described (Wang, et al., 2021). For example, the IC50 of mD1.22 and Nb-172 against 92UG024 was about 9.0 nM and 207.7 nM, respectively, so they were mixed at a ratio of 1:23, followed by a second round of testing the inhibitory activity against 92UG024. The mixture of mD1.22 and nanobody was diluted and incubated with 100TCID$_{50}$ of HIV-1 at 37 °C for 0.5 h before MT-2 cells or CEMx174 5.25 M7 cells were added to the mixture. After incubation at 37 °C for 12 h, the supernatants were replaced with RPMI-1640 medium with 10 % FBS. After an additional 4 days, the cell supernatant was collected and treated with 5 % TritonX-100, and p24 antigen was detected by ELISA, as previously described (Lu, et al., 2012). Briefly, human HIV-1 IgG was coated on wells of a 96-well polystyrene plate at 5 µg/mL at 4 °C overnight, and then the plate was blocked with 5 % nonfat milk at 37 °C for 2 h. The collected supernatants were added to the plate and incubated at 37 °C for 1 h. Then, mouse anti-p24 monoclonal antibody 183 was added and incubated for another 1 h. Following this, HRP-conjugated Rabbit anti-mouse IgG (Dako, Denmark) was used to detect p24 antigen levels. TMB and H_2O_2 were used to visualize the enzyme-linked reaction according to the previous description.

2.7. Inactivation of HIV-1 virions

The effect of Nb-172 on mD1.22-mediated HIV-1 inactivation activity was determined, as previously described (Su, et al., 2017). Briefly, Nb-172 and mD1.22 were serially diluted 1:4 before mixing with 500 TCID$_{50}$ HIV-1 at equivalent volume and incubated at 4 °C for 1 h. Then, PEG-6000 was added to the mixture at a final concentration of 3 % to precipitate the virus at 4 °C for 1 h. After that, the mixture was centrifuged at 13,000 rpm for 30 min and washed 3 times with 3 % PEG containing 10 mg/mL BSA. The virus pellet was resuspended with RPMI-1640 medium and cultured with MT-2 cells (X4 virus) or CEMx174 5.25 M7 cells (R5 virus). After a 5-day incubation, the supernatants were collected, treated with 5 % TritonX-100, and tested for p24 expression level with ELISA as described previously.

2.8. Bio-layer interferometry (BLI)

The binding kinetics between Nb-172 and N63-trimer protein was measured by BLI on an Octet-RED96 (ForteBio, USA). N63-trimer-Fc was loaded onto anti-human IgG Fc capture-coated (AHC) biosensors at 10 µg/mL. Nb-172 and D5 scFv were serially diluted 1:3, starting at 1 µM, with PBST. After association for 300 s, the antigen-immobilized sensors were immersed in PBST for another 300 s for dissociation. All curves were fitted with 1:1 binding model, and K_D values were determined, but only if R2 values > 95 % confidence level.

2.9. Native polyacrylamide gel electrophoresis (N-PAGE)

The blocking effect of Nb172 on the formation of 6-HB by C34 and N36 was confirmed by N-PAGE as previously described (Yu, et al., 2013). Serially diluted Nb-172 was incubated with an equal volume of N36 peptide (20 µM) at 37 °C for 1 h. C34 peptide was then added to the mixture at a final concentration of 5 µM and incubated at 37 °C for 0.5 h. Then the mixture was loaded on a Tris-glycine gel, followed by electrophoresis for 2 h before visualization by Coomassie blue.

2.10. Statistical analysis

Statistical analysis was conducted by GraphPad Prism 9.0. Statistical significance between different groups was established using two-way ANOVA, and a *p*-value below 0.05 was considered significant; * $p < 0.05$.

2.11. Combination index (CI)

The CI of mD1.22 and Nb-172 against different HIV-1 strains was calculated using the CalcuSyn program (Biosoft, Ferguson, MO, USA). CI < 1 represents the effect of synergism, and $0.1 < CI < 0.3$, $0.3 < CI < 0.7$, $0.7 < CI < 0.85$, and $0.85 < CI < 0.9$ indicate strong synergism, synergism, moderate synergism, and slight synergism, respectively.

3. Results

3.1. Isolation of HIV-1 gp41 NHR-binding nanobodies

To obtain nanobodies targeting HIV-1 gp41 NHR, we used covNHR-VQ, a reported engineered trimeric protein based on NHR sequence

(Jurado, et al., 2019) to immunize alpaca (Fig. 1A) based on a 9-week immunization schedule. The immunogen covNHR-VQ was successfully expressed in *E. coli* and purified (Fig. 1B). After the 4th immunization, high levels of covNHR-VQ-specific antibodies were detected in alpaca serum (Fig. 1C) and showed a significant difference compared to pre-immunization levels. To detect whether the immunized alpaca produced HIV-1 neutralizing antibodies, we detected the HIV-1 neutralizing titers in alpaca serum. Neutralization titer of alpaca serum against HIV-1 laboratory-adapted strain Bal (R5) was not detected at 37 °C (Fig. 1D), which could be attributed to the natural heavy chain-only antibody (HCAb) with a molecular weight of approximately 100 KD in alpaca that could not penetrate the steric hindrance caused by

conformational changes during the fusion process (Hamers-Casterman, et al., 1993). Previously, Golding et al. (Golding, et al., 2002) demonstrated that a temperature of 31.5 °C could slow down the transition of gp41 from the pre-hairpin intermediate state to the post-hairpin fusion state, which allowed accumulation of more advanced gp41 fusion intermediates. As suspected, the immunized alpaca serum did show neutralizing activity at 31.5 °C (Fig. 1E). Thus, we isolated the peripheral blood mononuclear cells (PBMCs) of alpaca, extracted total RNA, and constructed a phage library against covNHR-VQ with a capacity of 1.02×10^9 clones (Fig. 1F). The positive phage was screened by three rounds of ELISA, and the sequences of nanobodies were compared and sorted. After removing similar sequences and performing
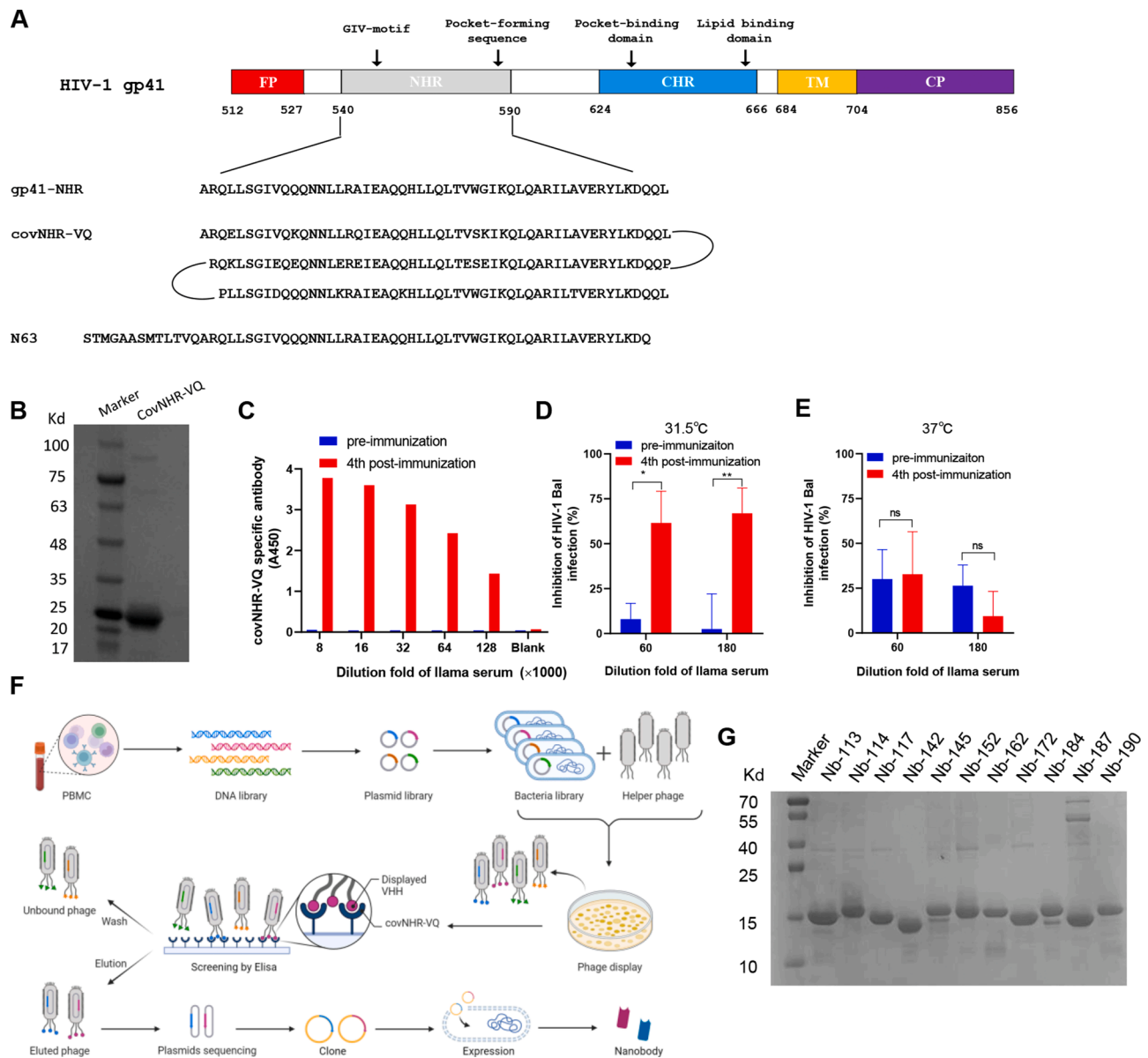
Fig. 1. Nanobodies targeting NHR were obtained by immunizing alpaca with NHR-trimer mimic covNHR-VQ. (A) Domain distribution of HIV-1 gp41 and sequences of NHR-derived proteins. HIV-1 gp41 is composed of 345 amino acid residues, corresponding to residues 512–856 of HXB2 gp160. It consists of an extracellular domain, a transmembrane domain (TM) and a cytoplasmic domain (CP). The extracellular domain of HIV gp41 contains three important functional domains: fusion peptide (FP), N-terminal heptapeptide repeat (NHR) and C-terminal heptapeptide repeat (CHR). GIV motif (aa 547–556) and pocket-forming sequence (aa 566–583) in the NHR and pocket-binding domain (aa 628–635) and lipid binding domain (aa 659–666) in the CHR are labeled. (B) Analysis of covNHR-VQ with SDS-PAGE. (C) The titer of covNHR-VQ-specific antibody in alpaca serum after 4 times immunization. (D-E) Neutralizing titer of alpaca serum against HIV-1 Bal at 37 °C and 31.5 °C. (F) Schematic illustration of phage display strategy to screen NHR-specific nanobodies. The total RNA of alpaca PBMCs was extracted to synthesize cDNA. Nanobody gene fragment was amplified by nested PCR and expressed in a phage library. The covNHR-VQ-specific nanobodies were screened through ELISA and expressed in *Bacillus*. (G) Analysis of nanobodies with SDS-PAGE. Biological replicates in one experiment were used for statistical analysis. Two-way ANOVA was used in the statistical analysis. * and NS mean $p < 0.05$ and no statistical significance, respectively.

complementary-determining region (CDR) analysis, 11 specific clones of different sequences were screened out. We successfully expressed these specific nanobodies using prokaryotic expression, which displayed dominant bands in the SDS-PAGE with a molecular weight of approximately 15 KD (Fig. 1G).

3.2. NHR-binding nanobodies showed neutralizing activity against HIV-1

To determine whether nanobodies could bind to the NHR trimer, we fused the trimerization motif of T4 bacteriophage fibritin-foldon to the C-terminus of NHR-derived peptide N63 to generate an N63-trimer, as previously described (Bi, et al., 2022). It contains all sequences of the gp41 NHR motif (Fig. 1A), which can better mimic the natural conformation of the NHR trimer. The affinity of nanobodies to the N63 trimeric protein was identified using ELISA. Most nanobodies showed concentration-dependent binding to the N63-trimer. However, some nanobodies, such as Nb-162, Nb-172, and Nb-187, exhibited much stronger affinity to the N63-trimer with no decrease in their binding ability observed within the detection concentration range (Fig. 2A). However, only Nb-117, Nb-145, Nb-162, Nb-172, Nb-187, and Nb-190 could neutralize HIV-1 Bal infection within the detection concentration range, while Nb-162 and Nb-172 showed the strongest neutralizing activity with IC_{50} (half maximal inhibitory concentration) values of 1.19 and 0.33 μM, respectively (Fig. 2B).

3.3. Nb-172 exhibited broad and potent neutralizing activity against HIV-1

To study the inhibitory spectrum of Nb-162 and Nb-172 on different HIV-1 stains, we evaluated the antiviral activity of Nb-162 and Nb-172 against pseudoviruses carrying Env of a panel of HIV-1 strains. Compared with D5 scFv, a single-chain antibody fragment targeting NHR (Miller, et al., 2005), both nanobodies showed a stronger ability to inhibit pseudovirus entry. Between the two, Nb-172 showed better neutralizing ability against HIV-1 pseudoviruses with IC_{50} of 0.15~1.59 μM (Table 1). Then, we evaluated the antiviral activity of nanobodies against some HIV-1 primary isolates, including 92UG024 (D, X4), 92UG029 (A, X4), and 93/BR/020 (F, X4/R5). Similar to D5 scFv, Nb-162 exhibited antiviral activity against all these HIV-1 clinical isolates, but Nb-172 could significantly suppress HIV-1 infection with an IC_{50} of 0.21–0.34 μM, approximately 3- to 5-fold more potency than that of D5 scFv (Fig. 3A-C). Next, we assessed the antiviral activity of Nb-172 against T20-resistant HIV-1 strains. As shown in Table 2, Nb-172 was highly effective against T20-resistant strains with IC_{50} ranging from 0.10 to 0.54 μM. These results demonstrate that Nb-172 exhibited potent and broadly neutralizing activity against HIV-1 pseudoviruses, HIV-1 primary isolates, and T20-resistant strains.

Table 1
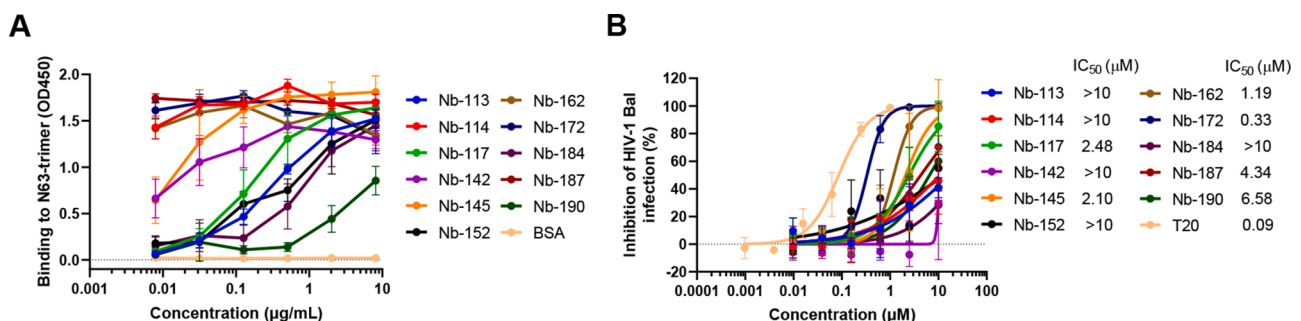Neutralizing activity of Nb-162 and Nb-172 against HIV-1 pseudoviruses.

strain	subtype	tier	IC_{50} (μM) Nb-162	IC_{50} (μM) Nb-172	IC_{50} (μM) D5 scFv
TRO_11	B	2	1.41	0.90	4.91
CH119	CRF07_BC	2	>5	1.59	>5
G clone 252	G	2	0.45	0.20	4.43
CRF02_AG clone 278	CRF02_AG	3	0.37	0.15	0.73
PVO clone 4	B	3	0.72	0.28	1.67
BJOX002000	CRF07_BC	–	2.52	0.88	3.87
HXB2	B	–	3.71	0.29	0.71

3.4. Combinatorial use of mD1.22 and Nb-172 exhibited synergism in inhibiting HIV-1 infection

Previous studies revealed the potential synergism between a gp120-inhibitor and a gp41-binding antibody when combined to inhibit HIV-1 infection (Wang, et al., 2021). MD1.22 is a soluble CD4 subunit D1 analog with high solubility and stability in a neutral environment, and it can inhibit a variety of HIV-1 strains in the low nanomole range (Chen, et al., 2014). Based on this finding, we reasoned that mD1.22 and Nb-172 used in combination might have the same result as the example above. Accordingly, we measured the inhibitory activity of mD1.22 and Nb-172 against HIV-1 clinical isolates. The results showed that mD1.22 and Nb-172 used in combination did exhibit a potent synergistic effect on inhibiting infection of different HIV-1 primary isolates with CI values of 0.24, 0.34, and 0.45, respectively. The IC_{50} values of mD1.22 and Nb-172 in combination against different HIV-1 strains increased from 2.03- to 24.75-fold and 2.02- to 33.69-fold, respectively (Table 3). These results indicate that the combined use of mD1.22 and Nb-172 can improve anti-HIV activity.

3.5. Combinatorial use of mD1.22 and Nb-172 exhibited synergism in inactivating HIV-1 virion

Although Nb-172 targeting the NHR can inhibit HIV-1 entry into the cell, it cannot inactivate cell-free HIV-1 virions. Notably, our previous study has shown that the gp41-targeting D5 scFv, in combination with a gp120-targeting protein mD1.22, could enhance the inactivation activity mediated by mD1.22 (Wang, et al., 2021). Similarly, here we found that the combination of Nb-172 in its combination with mD1.22 could also enhance the inactivation activity of mD1.22, with the half-maximal effective concentration (EC_{50}) of mD1.22 in the combination of 0.78, 3.47, and 0.15 nM, respectively, in inactivating HIV-1 92UG024, 92UG029, and 93/BR/020 virions, with EC_{50} values of mD1.22 alone of 2.07, 9.47, and 0.40 nM, about 1.7-fold more potent than mD1.22 alone, while Nb-172 alone had no inactivation activity at the concentration up to 250 nM (Fig. 4A-C). These results provide evidence that the combinatorial use of the gp41-binding nanobody Nb-172 and gp120-binding protein mD1.22 could enhance the total inactivation effect on cell-free HIV-1 virions.

Fig. 2. NHR affinity and anti-HIV-1 activity of nanobodies. (A) Binding ability of nanobodies to N63-trimer. (B) Antiviral activity of nanobodies against HIV-1 laboratory-adapted strain Bal.
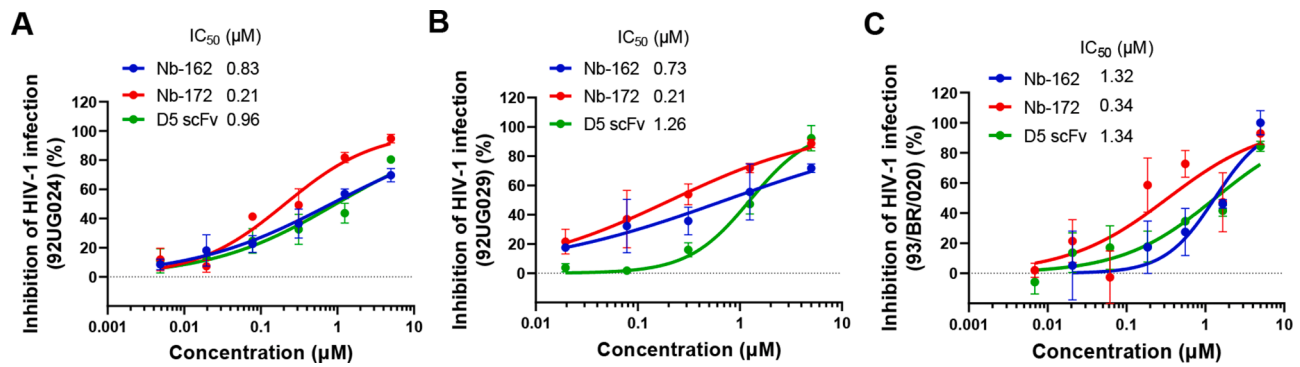
Fig. 3. Antiviral activity of Nb-162 and Nb-172 against HIV-1 primary isolates. Neutralizing activity of nanobodies against infection by HIV-1 clinical isolates 92UG024 (A), 92UG029 (B), and 93/BR/020 (C).

Table 2
Neutralizing activity of Nb-172 against T20-resistant HIV-1 strains.

Virus strain	IC_{50} (Mean ± SD) (μM)		
	Nb-162	Nb-172	T20
WT	>10	0.20±0.05	0.01±0.00
N42T, N43K	1.43±0.44	0.54±0.13	>1
V38E, N42S	2.29±1.72	0.10±0.01	>1
V38A, N42T	>10	0.24±0.13	0.60±0.28

Notes: WT, HIV-1 NL4–3 D36G.

3.6. Nb-172 inhibited 6-HB formation by binding to the hydrophobic pocket of NHR

To find the potential antiviral mechanism of Nb-172, we first used BLI to determine the binding ability of Nb-172 to the gp41 NHR-trimer. Nb-172 showed potent binding ability to N63-trimer, compared to that of D5 scFv, with K_D value of 24.5 nM (Fig. 5A and B). Further, we examined the binding ability of Nb-172 to IQN17, a trimeric peptide that can present the hydrophobic coiled-coil pocket of gp41 NHR, as described previously (Eckert, et al., 1999). D5 scFv, which targets the highly conserved gp41 NHR hydrophobic pocket (Miller, et al., 2005),

was used as a control. The binding of Nb-172 to IQN17 peptide was concentration-dependent, but compared with D5 scFv, Nb-172 displayed a relatively weaker affinity to IQN17 (Fig. 5C), suggesting that the target of Nb-172 may not completely coincide with that of D5 scFv. Then, we evaluated the ability of Nb-172 and CHR-derived peptides C34 and T20 to competitively bind to HIV-1 gp41 NHR. As shown in Fig. 5D, C34 peptide blocked the binding of Nb-172 to N63-timer in a concentration-dependent manner, suggesting that the binding epitope of Nb-172 and C34 may overlap. However, the presence of T20 had little effect on the binding of Nb-172 to N63-trimer, indicating that the key binding region of Nb-172 consists of residues in the hydrophobic pocket of NHR, rather than the main binding site of T20 (Fig. 1E), corresponding to the result in which Nb-172 showed neutralizing activity against T20-resistant HIV-1 strains with mutations in NHR. These results indicate that Nb-172 can competitively bind to NHR, preventing its interaction with CHR to form the 6-HB. Not surprisingly, native PAGE results confirmed that Nb-172 could block the interaction of N36 and C34 peptides to form 6-HB (Fig. S1).

Finally, AlphaFold3 (Abramson, et al., 2024) was used to predict the structure of the N63 trimer in complex with Nb-172. As shown in Fig. 5F, Nb-172 binds to residues L29-A51 of N63 (557–579 of gp41 NHR) mainly through its CDR2 and CDR3. In addition, Nb-172 can block the

Table 3
Combinatorial use of mD1.22 and Nb-172 to inhibit infection by HIV-1 primary isolates.

Virus strain	CI	mD1.22			Nb-172		
		IC_{50} (nM)		Fold of enhancement	IC_{50} (nM)		Fold of enhancement
		Alone	In combination		Alone	In combination	
92UG024	0.24	9.0	1.2	6.50	207.7	27.6	6.53
92UG029	0.34	10.0	3.3	2.03	211.0	69.8	2.02
93/BR/020	0.45	10.3	0.4	24.75	336.5	9.7	33.69
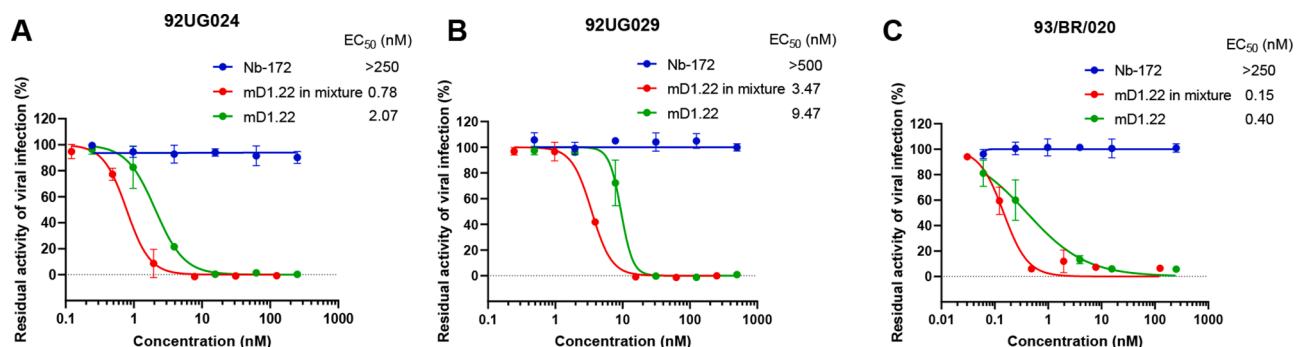
Fig. 4. Inactivation activity of mD1.22 and Nb-172 in combination against HIV-1 virions. Inactivation activity of Nb-172 and mD1.22 against cell-free HIV-1 92UG024 (A), 92UG029 (B), and 93/BR/020 (C) virions.
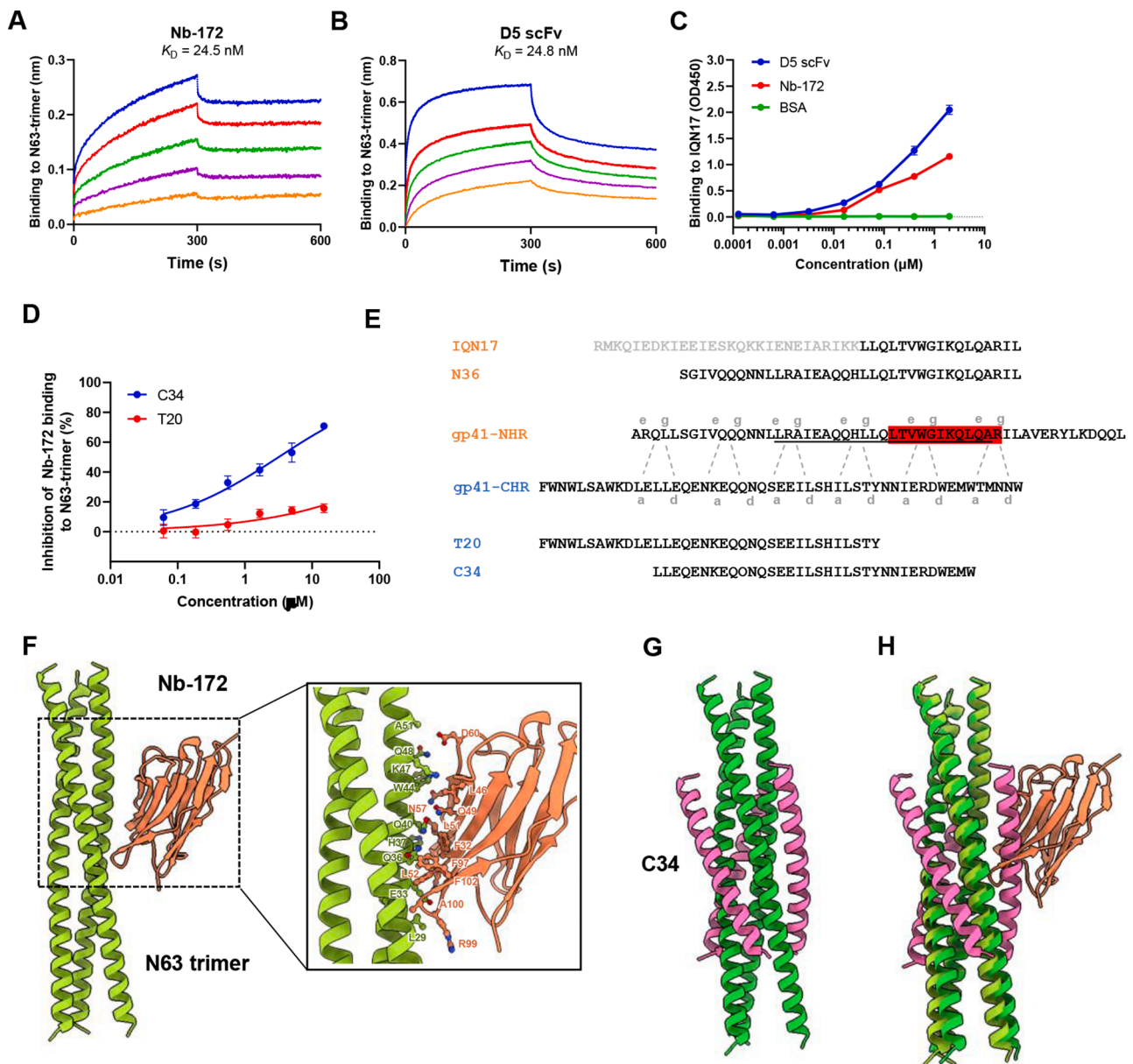
Fig. 5. Nb-172 inhibited the formation of 6-HB by binding to the hydrophobic pocket of NHR. (A-B) N63-trimer affinity of Nb-172 and D5 scFv. (C) Binding ability of Nb-172 to IQN17 peptide. (D) Nb-172 competitively binds to N63-trimer with CHR-derived peptides. (E) Schematic representation of interaction between gp41 NHR and CHR. The CHR sequence has been reversed to illustrate the NHR-CHR interactions through residues at the *a* and *d* sites and the *e* and *g* sites. Residues that make up the hydrophobic pocket are highlighted in red. The potential binding site of Nb172 is represented by underscore. (F) Predicted structure of the N63-trimer in complex with Nb-172 by AlphaFold3. (G) Structure of N63-trimer and C34. (H) Binding region of Nb-172 overlaps with that of C34.

NHR- CHR interface by binding to the region on the N63-trimer that overlaps with the C34 peptide (Fig. 5G and 5H), coinciding with the above results. Notably, in the complex structure, many residues within the binding region exhibited pLDDT (predicted local distance difference test) scores above 70, indicating a high level of model confidence in the predictions made by AlphaFold3. All these results suggest that Nb-172 can competitively bind to the NHR hydrophobic pocket and interfere with the formation of 6-HB.

4. Discussion

Gp41 is a promising target for HIV vaccine development and antibody drug design by the highly conserved sequences of FP, MPER, and NHR regions. These conserved regions of gp41 play a critical role in conformational changes, transforming the natural pre-fusion gp41 structure into post-fusion conformation (Caillat, et al., 2020). However, most antibodies against gp41 induced during natural infection are non-neutralizing (Tomaras, et al., 2008). Some monoclonal antibodies targeting the MPER of gp41 have shown potent anti-HIV-1 activity, such as 2F5, 4E10, and 10E8 (Huang, et al., 2012; Yang, et al., 2013), but it is hard to induce these bNAbs by immunization with immunogens containing the MPER sequence (Liu, et al., 2018). Apparently, the recently reported MPER peptide-liposome immunization strategy is expected to change this situation (Williams, et al., 2024). Meanwhile, few successful immunization cases are known to effectively stimulate specific antibodies targeting NHR.

Nelson et al. (Nelson, et al., 2008) obtained mAb 8K8-scFv by immunizing rabbits with an NHR coiled-coil mimic, N35_{CCG}-N13, which had anti-HIV-1 activity, but did not inhibit the formation of 6-HB. In spite of its limited potency, this work does confirm that neutralizing Abs

can be elicited by NHR trimer alone. The structure of the HIV-1 gp41 post-fusion bundle shows a prominent hydrophobic pocket in the NHR trimer, consisting of seven discontinuous residues, including L568, V570, W571, K574, Q575, Q577, and R579 (Bruun, et al., 2023; Chan, et al., 1997). The hydrophobic pocket region is essential for the binding of CHR and NHR to form a hairpin-like six-helix bundle in which amino acid mutations can seriously increase the infectivity of HIV-1, thus making it an ideal conserved target for antibody drug design (Cao, et al., 1993). However, it is hard for IgG molecules to break the steric hindrance generated by conformational alteration in the fusion process to then bind tightly to NHR (Corti, et al., 2010).

However, in this study, we reported a nanobody, termed as Nb-172, targeting the pocket region of gp41 NHR by immunizing alpaca with an NHR-trimer mimic. Nb-172 shows broadly neutralizing ability against HIV-1 pseudoviruses with IC_{50} that ranges from 0.15 to 1.59 μM and potent antiviral activity against HIV-1 primary isolates with IC_{50} that ranges from 0.21~0.34 μM. Moreover, Nb-172 was highly effective against T20-resistant strains with IC_{50} ranging from 0.10 to 0.54 μM, showing more potency than D5 scFv (Miller, et al., 2005). The binding of CD4 mimics to gp120 CD4-binding site (CD4bs) can cause conformational changes to expose co-receptor binding sites and induce the formation of gp41 pre-hairpin fusion intermediate with NHR hydrophobic groove and pocket exposed (Haim, et al., 2009), and the gp41-targeting peptide or scFv can enhance the inactivation activity mediated by the gp120-targeting protein (Wang, et al., 2021, 2022). Here, we found that combinatorial use of CD4 mimic mD1.22 and nanobody Nb-172 exhibited a significant synergistic effect in that the IC_{50} values of mD1.22 and Nb-172 in combination against different HIV-1 strains were significantly enhanced, increasing from 2.03- to 24.75-fold, and 2.02- to 33.69-fold, respectively. Nb-172 also promoted the efficiency of mD1.22 to inactivate cell-free virions, with EC_{50} values increasing by 1.65- to 1.73-fold. In addition, C34 blocked the binding of N172 to N63-trimer in a concentration-dependent manner, indicating that the binding epitope of Nb-172 and C34 may overlap. Previously, Strokappe et al. (Strokappe, et al., 2012, 2019) screened a nanobody, termed as 2E7, targeting gp41 NHR by immunizing alpaca with gp140, and it exhibited anti-HIV activity similar to that of Nb-172. However, unlike 2E7, Nb-172 binds with the region comprised of residues 557 to 579, containing a hydrophobic pocket of NHR, while 2E7 binds to residues 583–596 outside the pocket region. Since the hydrophobic pocket is crucial for 6-HB formation, Nb-172 stands out as a promising candidate for development as a therapeutic antibody.

In summary, we are the first to report an alpaca-derived single-domain antibody Nb-172 targeting the hydrophobic pocket region of gp41 NHR, which shows broad anti-HIV-1 activity and exhibits synergism in combinatorial use with mD1.22. We acknowledge some limitations in this study. For example, the accurate target sites of Nb-172 need to be further analyzed by the crystal structure obtained from X-ray diffraction. As a nanobody, Nb-172 demonstrates strong immunogenicity. Therefore, further humanization is necessary to ensure the safety and efficacy of therapeutics.

Funding

CRediT authorship contribution statement

Lujia Sun: Methodology, Formal analysis, Data curation, Writing – original draft. **Bo Chen:** Methodology, Data curation. **Xianbo Liu:** Methodology, Data curation. **Yun Zhu:** Methodology, Formal analysis, Data curation. **Guangxu Zhang:** Methodology, Supervision. **Xiaoxing Liang:** Methodology, Supervision. **Lixiao Xing:** Methodology, Supervision. **Wei Xu:** Methodology, Supervision. **Shibo Jiang:** Conceptualization, Funding acquisition, Supervision, Writing – review & editing.

Xinling Wang: Conceptualization, Methodology, Formal analysis, Data curation, Supervision, Writing – review & editing.

Declaration of competing interest

Xinling Wang, Bo Chen, Shibo Jiang, Lujia Sun, and Xianbo Liu are inventors in a patent application related to Nb-172 in this study. Other authors declare that they have no conflict of interest.

Data availability

Data will be made available on request.

Acknowledgments

Supplementary materials

Supplementary material associated with this article can be found, in the online version, at doi:10.1016/j.crmicr.2024.100263.

References

Abramson, J., Adler, J., Dunger, J., Evans, R., Green, T., Pritzel, A., Ronneberger, O., Willmore, L., Ballard, A.J., Bambrick, J., Bodenstein, S.W., Evans, D.A., Hung, C.C., O'Neill, M., Reiman, D., Tunyasuvunakool, K., Wu, Z., Zemgulyte, A., Arvaniti, E., Beattie, C., Bertolli, O., Bridgland, A., Cherepanov, A., Congreve, M., Cowen-Rivers, A.I., Cowie, A., Figurnov, M., Fuchs, F.B., Gladman, H., Jain, R., Khan, Y.A., Low, C.M.R., Perlin, K., Potapenko, A., Savy, P., Singh, S., Stecula, A., Thillaisundaram, A., Tong, C., Yakneen, S., Zhong, E.D., Zielinski, M., Zidek, A., Bapst, V., Kohli, P., Jaderberg, M., Hassabis, D., Jumper, J.M., 2024. Accurate structure prediction of biomolecular interactions with AlphaFold 3. Nature 630, 493–500.

Bi, W., Chen, G., Dang, B., 2022. Novel engineered SARS-CoV-2 HR1 trimer exhibits improved potency and broad-spectrum activity against SARS-CoV-2 and its variants. J. Virol. 96, e0068122.

Bruun, T.U.J., Tang, S., Erwin, G., Deis, L., Fernandez, D., Kim, P.S., 2023. Structure-guided stabilization improves the ability of the HIV-1 gp41 hydrophobic pocket to elicit neutralizing antibodies. J. Biol. Chem. 299, 103062.

Caillat, C., Guilligay, D., Sulbaran, G., Weissenhorn, W., 2020. Neutralizing antibodies targeting HIV-1 gp41. Viruses 12.

Cao, J., Bergeron, L., Helseth, E., Thali, M., Repke, H., Sodroski, J., 1993. Effects of amino acid changes in the extracellular domain of the human immunodeficiency virus type 1 gp41 envelope glycoprotein. J. Virol. 67, 2747–2755.

Caskey, M., Klein, F., Nussenzweig, M.C., 2019. Broadly neutralizing anti-HIV-1 monoclonal antibodies in the clinic. Nat. Med. 25, 547–553.

Chan, D.C., Fass, D., Berger, J.M., Kim, P.S., 1997. Core structure of gp41 from the HIV envelope glycoprotein. Cell 89, 263–273.

Chen, W., Feng, Y., Prabakaran, P., Ying, T., Wang, Y., Sun, J., Macedo, C.D., Zhu, Z., He, Y., Polonis, V.R., Dimitrov, D.S., 2014. Exceptionally potent and broadly cross-reactive, bispecific multivalent HIV-1 inhibitors based on single human CD4 and antibody domains. J. Virol. 88, 1125–1139.

Corti, D., Langedijk, J.P., Hinz, A., Seaman, M.S., Vanzetta, F., Fernandez-Rodriguez, B. M., Silacci, C., Pinna, D., Jarrossay, D., Balla-Jhagjhoorsingh, S., Willems, B., Zekveld, M.J., Dreja, H., O'Sullivan, E., Pade, C., Orkin, C., Jeffs, S.A., Montefiori, D. C., Davis, D., Weissenhorn, W., McKnight, A., Heeney, J.L., Sallusto, F., Sattentau, Q. J., Weiss, R.A., Lanzavecchia, A., 2010. Analysis of memory B cell responses and isolation of novel monoclonal antibodies with neutralizing breadth from HIV-1-infected individuals. PLoS One 5, e8805.

Cunningham, S., Piedra, P.A., Martinon-Torres, F., Szymanski, H., Brackeva, B., Dombrecht, E., Detalle, L., Fleurinck, C., group R.s., 2021. Nebulised ALX-0171 for respiratory syncytial virus lower respiratory tract infection in hospitalised children: a double-blind, randomised, placebo-controlled, phase 2b trial. Lancet Respir Med 9, 21–32.

De Genst, E., Silence, K., Decanniere, K., Conrath, K., Loris, R., Kinne, J., Muyldermans, S., Wyns, L., 2006. Molecular basis for the preferential cleft recognition by dromedary heavy-chain antibodies. Proc. Natl. Acad. Sci. USA 103, 4586–4591.

Eckert, D.M., Malashkevich, V.N., Hong, L.H., Carr, P.A., Kim, P.S., 1999. Inhibiting HIV-1 entry: discovery of d-peptide inhibitors that target the gp41 coiled-coil pocket. Cell 99, 103–115.

Eckert, D.M., Shi, Y., Kim, S., Welch, B.D., Kang, E., Poff, E.S., Kay, M.S., 2008. Characterization of the steric defense of the HIV-1 gp41 N-trimer region. Protein Sci. 17, 2091–2100.

Finzi, D., Blankson, J., Siliciano, J.D., Margolick, J.B., Chadwick, K., Pierson, T., Smith, K., Lisziewicz, J., Lori, F., Flexner, C., Quinn, T.C., Chaisson, R.E., Rosenberg, E., Walker, B., Gange, S., Gallant, J., Siliciano, R.F., 1999. Latent infection of CD4+ T cells provides a mechanism for lifelong persistence of HIV-1, even in patients on effective combination therapy. Nat. Med. 5, 512–517.

Golding, H., Zaitseva, M., de Rosny, E., King, L.R., Manischewitz, J., Sidorov, I., Gorny, M.K., Zolla-Pazner, S., Dimitrov, D.S., Weiss, C.D., 2002. Dissection of human immunodeficiency virus type 1 entry with neutralizing antibodies to gp41 fusion intermediates. J. Virol. 76, 6780–6790.

3rd Haim, H., Si, Z., Madani, N., Wang, L., Courter, J.R., Princiotto, A., Kassa, A., DeGrace, M., McGee-Estrada, K., Mefford, M., Gabuzda, D., Smith, A.B., Sodroski, J., 2009. Soluble CD4 and CD4-mimetic compounds inhibit HIV-1 infection by induction of a short-lived activated state. PLoS Pathog. 5, e1000360.

Halper-Stromberg, A., Lu, C.L., Klein, F., Horwitz, J.A., Bournazos, S., Nogueira, L., Eisenreich, T.R., Liu, C., Gazumyan, A., Schaefer, U., Furze, R.C., Seaman, M.S., Prinjha, R., Tarakhovsky, A., Ravetch, J.V., Nussenzweig, M.C., 2014. Broadly neutralizing antibodies and viral inducers decrease rebound from HIV-1 latent reservoirs in humanized mice. Cell 158, 989–999.

Hamers-Casterman, C., Atarhouch, T., Muyldermans, S., Robinson, G., Hamers, C., Songa, E.B., Bendahman, N., Hamers, R., 1993. Naturally occurring antibodies devoid of light chains. Nature 363, 446–448.

Hanke, L., Vidakovics Perez, L., Sheward, D.J., Das, H., Schulte, T., Moliner-Morro, A., Corcoran, M., Achour, A., Karlsson Hedestam, G.B., Hallberg, B.M., Murrell, B., McInerney, G.M., 2020. An alpaca nanobody neutralizes SARS-CoV-2 by blocking receptor interaction. Nat. Commun. 11, 4420.

Huang, J., Ofek, G., Laub, L., Louder, M.K., Doria-Rose, N.A., Longo, N.S., Imamichi, H., Bailer, R.T., Chakrabarti, B., Sharma, S.K., Alam, S.M., Wang, T., Yang, Y., Zhang, B., Migueles, S.A., Wyatt, R., Haynes, B.F., Kwong, P.D., Mascola, J.R., Connors, M., 2012. Broad and potent neutralization of HIV-1 by a gp41-specific human antibody. Nature 491, 406–412.

Jurado, S., Cano-Munoz, M., Morel, B., Standoli, S., Santarossa, E., Moog, C., Schmidt, S., Laumond, G., Camara-Artigas, A., Conejero-Lara, F., 2019. Structural and Thermodynamic Analysis of HIV-1 Fusion Inhibition Using Small gp41 Mimetic Proteins. J. Mol. Biol. 431, 3091–3106.

Liu, H., Su, X., Si, L., Lu, L., Jiang, S., 2018. The development of HIV vaccines targeting gp41 membrane-proximal external region (MPER): challenges and prospects. Protein Cell 9, 596–615.

Liu, M., Li, L., Jin, D., Liu, Y., 2021. Nanobody-A versatile tool for cancer diagnosis and therapeutics. Wiley Interdiscip. Rev. Nanomed. Nanobiotechnol. 13, e1697.

Lu, L., Pan, C., Li, Y., Lu, H., He, W., Jiang, S., 2012. A bivalent recombinant protein inactivates HIV-1 by targeting the gp41 prehairpin fusion intermediate induced by CD4 D1D2 domains. Retrovirology 9, 104.

Lu, M., Kim, P.S., 1997. A trimeric structural subdomain of the HIV-1 transmembrane glycoprotein. J. Biomol. Struct. Dyn. 15, 465–471.

Miller, M.D., Geleziunas, R., Bianchi, E., Lennard, S., Hrin, R., Zhang, H., Lu, M., An, Z., Ingallinella, P., Finotto, M., Mattu, M., Finnefrock, A.C., Bramhill, D., Cook, J., Eckert, D.M., Hampton, R., Patel, M., Jarantow, S., Joyce, J., Ciliberto, G., Cortese, R., Lu, P., Strohl, W., Schleif, W., McElhaugh, M., Lane, S., Lloyd, C., Lowe, D., Osbourn, J., Vaughan, T., Emini, E., Barbato, G., Kim, P.S., Hazuda, D.J., Shiver, J.W., Pessi, A., 2005. A human monoclonal antibody neutralizes diverse HIV-1 isolates by binding a critical gp41 epitope. Proc. Natl. Acad. Sci. USA 102, 14759–14764.

Mouquet, H., Scharf, L., Euler, Z., Liu, Y., Eden, C., Scheid, J.F., Halper-Stromberg, A., Gnanapragasam, P.N., Spencer, D.I., Seaman, M.S., Schuitemaker, H., Feizi, T., Nussenzweig, M.C., Bjorkman, P.J., 2012. Complex-type N-glycan recognition by potent broadly neutralizing HIV antibodies. Proc. Natl. Acad. Sci. USA 109, E3268–E3277.

Nelson, J.D., Kinkead, H., Brunel, F.M., Leaman, D., Jensen, R., Louis, J.M., Maruyama, T., Bewley, C.A., Bowdish, K., Clore, G.M., Dawson, P.E., Frederickson, S., Mage, R.G., Richman, D.D., Burton, D.R., Zwick, M.B., 2008. Antibody elicited against the gp41 N-heptad repeat (NHR) coiled-coil can neutralize HIV-1 with modest potency but non-neutralizing antibodies also bind to NHR mimetics. Virology 377, 170–183.

Palella Jr., F.J., Delaney, K.M., Moorman, A.C., Loveless, M.O., Fuhrer, J., Satten, G.A., Aschman, D.J., Holmberg, S.D., 1998. Declining morbidity and mortality among patients with advanced human immunodeficiency virus infection. HIV Outpatient Study Investigators. N. Engl. J. Med. 338, 853–860.

Sabin, C., Corti, D., Buzon, V., Seaman, M.S., Lutje Hulsik, D., Hinz, A., Vanzetta, F., Agatic, G., Silacci, C., Mainetti, L., Scarlatti, G., Sallusto, F., Weiss, R., Lanzavecchia, A., Weissenhorn, W., 2010. Crystal structure and size-dependent neutralization properties of HK20, a human monoclonal antibody binding to the highly conserved heptad repeat 1 of gp41. PLoS Pathog. 6, e1001195.

Sarker, S.A., Jakel, M., Sultana, S., Alam, N.H., Bardhan, P.K., Chisti, M.J., Salam, M.A., Theis, W., Hammarstrom, L., Frenken, L.G., 2013. Anti-rotavirus protein reduces stool output in infants with diarrhea: a randomized placebo-controlled trial. Gastroenterology 145 (740–748), e748.

Scheid, J.F., Mouquet, H., Ueberheide, B., Diskin, R., Klein, F., Oliveira, T.Y., Pietzsch, J., Fenyo, D., Abadir, A., Velinzon, K., Hurley, A., Myung, S., Boulad, F., Poignard, P., Burton, D.R., Pereyra, F., Ho, D.D., Walker, B.D., Seaman, M.S., Bjorkman, P.J., Chait, B.T., Nussenzweig, M.C., 2011. Sequence and structural convergence of broad and potent HIV antibodies that mimic CD4 binding. Science 333, 1633–1637.

Simon, V., Ho, D.D., Abdool Karim, Q., 2006. HIV/AIDS epidemiology, pathogenesis, prevention, and treatment. Lancet 368, 489–504.

Strokappe, N., Szynol, A., Aasa-Chapman, M., Gorlani, A., Forsman Quigley, A., Hulsik, D.L., Chen, L., Weiss, R., de Haard, H., Verrips, T., 2012. Llama antibody fragments recognizing various epitopes of the CD4bs neutralize a broad range of HIV-1 subtypes A, B and C. PLoS One 7, e33298.

Strokappe, N.M., Hock, M., Rutten, L., McCoy, L.E., Back, J.W., Caillat, C., Haffke, M., Weiss, R.A., Weissenhorn, W., Verrips, T., 2019. Super Potent Bispecific Llama VHH Antibodies Neutralize HIV via a Combination of gp41 and gp120 Epitopes. Antibodies (Basel) (8).

Su, S., Zhu, Y., Ye, S., Qi, Q., Xia, S., Ma, Z., Yu, F., Wang, Q., Zhang, R., Jiang, S., Lu, L., 2017. Creating an artificial tail anchor as a novel strategy to enhance the potency of peptide-based HIV fusion inhibitors. J. Virol. 91.

Tomaras, G.D., Yates, N.L., Liu, P., Qin, L., Fouda, G.G., Chavez, L.L., Decamp, A.C., Parks, R.J., Ashley, V.C., Lucas, J.T., Cohen, M., Eron, J., Hicks, C.B., Liao, H.X., Self, S.G., Landucci, G., Forthal, D.N., Weinhold, K.J., Keele, B.F., Hahn, B.H., Greenberg, M.L., Morris, L., Karim, S.S., Blattner, W.A., Montefiori, D.C., Shaw, G. M., Perelson, A.S., Haynes, B.F., 2008. Initial B-cell responses to transmitted human immunodeficiency virus type 1: virion-binding immunoglobulin M (IgM) and IgG antibodies followed by plasma anti-gp41 antibodies with ineffective control of initial viremia. J. Virol. 82, 12449–12463.

Wang, X., Cao, M., Wu, Y., Xu, W., Wang, Q., Ying, T., Lu, L., Jiang, S., 2021. Synergistic effect by combining a gp120-binding protein and a gp41-binding antibody to inactivate HIV-1 Virions and Inhibit HIV-1 Infection. Molecules 26.

Wang, X., Xu, W., Liu, Z., Wu, Y., Wang, Q., Cao, M., Ying, T., He, N., Lu, L., Jiang, S., 2022. A toxin-conjugated recombinant protein targeting gp120 and gp41 for Inactivating HIV-1 Virions and killing latency-reversing agent-reactivated latent cells. mBio 13, e0338421.

Weissenhorn, W., Dessen, A., Harrison, S.C., Skehel, J.J., Wiley, D.C., 1997. Atomic structure of the ectodomain from HIV-1 gp41. Nature 387, 426–430.

Williams, W.B., Alam, S.M., Ofek, G., Erdmann, N., Montefiori, D.C., Seaman, M.S., Wagh, K., Korber, B., Edwards, R.J., Mansouri, K., Eaton, A., Cain, D.W., Martin, M., Hwang, J., Arus-Altuz, A., Lu, X., Cai, F., Jamieson, N., Parks, R., Barr, M., Foulger, A., Anasti, K., Patel, P., Sammour, S., Parsons, R.J., Huang, X., Lindenberger, J., Fetics, S., Janowska, K., Niyongabo, A., Janus, B.M., Astavans, A., Fox, C.B., Mohanty, I., Evangelous, T., Chen, Y., Berry, M., Kirshner, H., Van Itallie, E., Saunders, K.O., Wiehe, K., Cohen, K.W., McElrath, M.J., Corey, L., Acharya, P., Walsh, S.R., Baden, L.R., Haynes, B.F., 2024. Vaccine induction of heterologous HIV-1-neutralizing antibody B cell lineages in humans. Cell.

Wittkop, L., Gunthard, H.F., de Wolf, F., Dunn, D., Cozzi-Lepri, A., de Luca, A., Kucherer, C., Obel, N., von Wyl, V., Masquelier, B., Stephan, C., Torti, C., Antinori, A., Garcia, F., Judd, A., Porter, K., Thiebaut, R., Castro, H., van Sighem, A. I., Colin, C., Kjaer, J., Lundgren, J.D., Paredes, R., Pozniak, A., Clotet, B., Phillips, A., Pillay, D., Chene, G., EuroCoord, C.s.g., 2011. Effect of transmitted drug resistance on virological and immunological response to initial combination antiretroviral therapy for HIV (EuroCoord-CHAIN joint project): a European multicohort study. Lancet Infect. Dis. 11, 363–371.

Wrapp, D., De Vlieger, D., Corbett, K.S., Torres, G.M., Wang, N., Van Breedam, W., Roose, K., van Schie, L., Team, V.-C.C.-R., Hoffmann, M., Pohlmann, S., Graham, B. S., Callewaert, N., Schepens, B., Saelens, X., McLellan, J.S., 2020. Structural basis for potent neutralization of betacoronaviruses by single-domain camelid antibodies. Cell 181 (1004–1015), e1015.

Yang, G., Holl, T.M., Liu, Y., Li, Y., Lu, X., Nicely, N.I., Kepler, T.B., Alam, S.M., Liao, H. X., Cain, D.W., Spicer, L., VandeBerg, J.L., Haynes, B.F., Kelsoe, G., 2013. Identification of autoantigens recognized by the 2F5 and 4E10 broadly neutralizing HIV-1 antibodies. J. Exp. Med. 210, 241–256.

Yu, F., Lu, L., Du, L., Zhu, X., Debnath, A.K., Jiang, S., 2013. Approaches for identification of HIV-1 entry inhibitors targeting gp41 pocket. Viruses 5, 127–149.

Zacharopoulou, P., Ansari, M.A., Frater, J., 2022. A calculated risk: evaluating HIV resistance to the broadly neutralising antibodies10-1074 and 3BNC117. Curr Opin HIV AIDS 17, 352–358.